

FINEL 337

An element for the analysis of transient exterior fluid–structure interaction problems using the FEM

L.F. Kallivokas and J. Bielak

Computational Mechanics Laboratory, Department of Civil Engineering, Carnegie Mellon University, Pittsburgh, PA 15213, USA

Abstract. A finite element-based procedure is presented for the solution directly in the time domain of transient problems involving structures submerged in an infinite acoustic fluid. A central component of the methodology employed herein, and presented in greater detail elsewhere, is a novel element that arises upon discretization of a high-order absorbing boundary condition introduced in the formulation of the fluid–structure interaction problem in order to render the computational domain finite. The new element is local in both time and space and is completely defined by a pair of symmetric stiffness and damping matrices. The familiar form of the discretized equations of motion for the structure is retained with its symmetry and sparseness intact. Standard temporal integration techniques can then be used for the solution of the equations. In this paper we present the methodology in a two-dimensional setting, together with numerical examples involving both circular and non-circular shells. Although the focus is on the time domain, the methodology is equally applicable in the frequency domain, thus providing a unified and efficient tool for the treatment of the exterior structural acoustics problem.

Introduction

The exterior structural acoustics problem, considered herein as a model case of fluid–structure interaction, typically involves the determination of the displacement and/or stress field of a structure submerged in an infinite acoustic fluid and the pressure field within the surrounding fluid, given an incident pressure field or radiation loading acting on the structure. The structure and the fluid are assumed to be linear and homogeneous¹, while the fluid is, in addition, assumed to be compressible and inviscid. In physical terms, as the structure vibrates while in contact with the fluid, there is a continuous interaction between the structure and the fluid; the structure feels the radiation loading due to the presence of the fluid which modifies the forces that act on the structure, hence giving rise to the coupling between the two media in a dynamic setting. In mathematical terms, one seeks the solution of the equations of elastodynamics for the structure, coupled with the scalar wave equation for the fluid, subject to the Sommerfeld radiation condition at infinity and appropriate transition conditions at the interface between the structure and the fluid.

In studying such a fluid–structure interaction problem, significant effort has been devoted to the analysis of the time-harmonic steady-state case. Frequency-domain approaches are predominant (See [1], and references therein), possibly for good reason, as the mathematical tools for such analyses are more rigorous and better understood. In addition, a primary difficulty associated with the numerical treatment of the infinite fluid, namely the appropriate

Correspondence to: L.F. Kallivokas, Department of Civil Engineering, Carnegie Mellon University, Pittsburgh, PA 15213, USA.

¹ Extension to structures with nonlinear material behavior is straightforward.

modeling of the Sommerfeld radiation condition, has thus far proven easier to implement in the frequency domain than in the time domain. Integral equation methods are prime representatives of the aforementioned ease, as the Green's functions involved in the formulation satisfy a priori the radiation condition. A further reason for the apparent popularity of such methodologies is the possibility of inverting, through appropriate Laplace or Fourier transforms, the frequency domain solutions back to the time domain and thus have a tool that provides the solution in the transient regime as well. The shortcomings of such approaches include limitations in their applicability at certain frequencies, unless particular corrective action is taken [2,3], and large computational cost associated with short wavelengths in the fluid compared to the dimensions of the structure; an extensive sweep of the frequency spectrum is required for any reasonably accurate solution in the time domain, while the size of the fully-populated unsymmetric matrices, which generally result from such methodologies, increases as the wave number increases.

Clearly, direct time domain approaches are needed not only as a natural alternative to the aforementioned indirect approaches, but also as the only viable means for tackling problems that involve structures that can behave inelastically. Within the realm of such methods, we mention the exact boundary integral formulation in terms of retarded potentials, which however suffers from the need to solve a dense system of equations at each time step. On the other hand, direct time domain approaches which rely on a field discretization scheme, such as the finite element method, require that the originally infinite domain be truncated for computations. To accommodate that need, a fictitious boundary is usually introduced at some distance from the structure. This particular idea gives rise to a class of methodologies that are based on absorbing (artificial) boundaries (See [4] for a review). Physically, the newly introduced boundary should simulate the behavior of the part of the infinite domain that has been excluded from the computational domain, in such a way that the solution obtained for the interior region of interest is, if possible, not affected, or, in practice, only slightly affected by its introduction. Mathematically, the artificial boundary should still render a well-posed problem. The boundary condition at the artificial boundary need be such that the governing field equations have a unique and stable solution. The methodology used herein relies precisely on the introduction of such an artificial boundary.

There is an exact boundary condition that holds at the interface between the computational domain and the exterior region, which is non-local in both space and time; that is, the motion at every point of the interface is coupled with that at all other points, and the response at any instant depends on the entire previous history. In mathematical terms the theoretical exact boundary condition is tantamount to an integral on the boundary (spatial non-locality) involving convolutions (temporal non-locality) of the boundary quantities under the first (spatial) integral sign. As the numerical implementation of such a condition entails a heavy computational burden both in terms of memory and time requirements, one aims at reducing the temporal or the spatial non-localities in an effort to render the problem solvable by present means.

An inherent difficulty with methodologies such as the above is the assurance of stability of the conditions and validity for the low end of the frequency spectrum, since the conditions are usually constructed using high frequency approximations. Geers [5] developed conditions, termed doubly asymptotic approximations (DAA), that are exact in both the low and high frequency limits and local in time but, unfortunately, non-local in space. A note should also be made of attempts to solve directly in the time domain the fluid–structure interaction problem. Pinsky et al. [6,7] used the Bayliss and Turkel [8] absorbing boundary conditions with finite elements, but there resulted a non-symmetric formulation that in two and three dimensions has been applied to Dirichlet and Neumann problems. Geers used the DAAs for the general problem, “a formidable task” as he put it in [9], but again the resulting

formulation suffers from the spatial non-locality of the conditions. Extensions to problems with inelastic interior structures using DAAs failed [10].

In devising a procedure for the solution of the fluid–structure interaction problem, within the family of methods that rely on artificial boundaries, one should aim for: (a) a stable high-order absorbing boundary condition so that sufficient accuracy for engineering applications is attained, (b) a small computational domain so that the associated computational cost is kept at a minimum, (c) locality in time so that extensive storage of time histories is avoided and the resulting equations of motion can be easily integrated in time and (d) locality in space such that standard finite element techniques that preserve the symmetry and the bandedness can be used. In this paper, we use a methodology that attempts to encompass all of these characteristics. We particularly aim at demonstrating the versatility of the method by showing the ease of incorporation into existing finite element codes. For the theoretical background we borrow heavily from the variational formulation presented in [11] for the particular case of circular cylindrical shells. Similarly, we follow Everstine's [12] introduction of a velocity potential to model the fluid and we use absorbing boundaries, borrowing from the work of Barry et al. [13] and Kallivokas et al. [14], to truncate the infinite domain to a finite one, while appropriate transition conditions are prescribed at the fluid–structure interface. The structure is described by the standard elastodynamics equations. Finite elements are used to model the structure, the fluid and the absorbing boundary. Upon discretization of the resulting weak form of the problem, the absorbing boundary is replaced by an impedance element, completely defined by a pair of symmetric damping and stiffness matrices, that can be easily attached to the adjoining fluid elements. The element is such that it can be readily incorporated into existing finite element libraries; to illustrate the validity of this claim, numerical results are presented for a non-circular shell using a specially modified version of a commercial code (ANSYS). Numerical results are shown also for a circular cylindrical shell in order to demonstrate the accuracy of the methodology through comparisons with exact solutions.

Mathematical formulation

Problem statement

Let Ω^e be a bounded domain occupied by a linear, isotropic, inhomogeneous elastic solid surrounded by a compressible, inviscid and homogeneous fluid occupying the exterior infinite

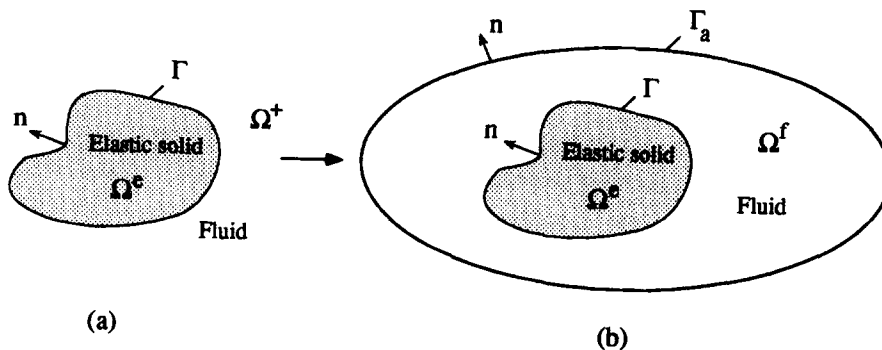


Fig. 1. (a) Fluid–structure interaction problem; (b) Modified problem.

region Ω^+ and let Γ be their interface [Fig. 1(a)]. Then,

$$\nabla \cdot \boldsymbol{\sigma}(\mathbf{u}_e) = \rho_e \ddot{\mathbf{u}}_e \quad \text{in } \Omega^e, \quad (1a)$$

$$\boldsymbol{\sigma}(\mathbf{u}_e) = \mathbf{C}[\mathbf{E}] = \mathbf{C}\left[\frac{1}{2}(\nabla \mathbf{u}_e + \nabla \mathbf{u}_e^T)\right] \quad \text{in } \Omega^e, \quad (1b)$$

$$\nabla^2 p^s = \frac{1}{c^2} \ddot{p}^s \quad \text{in } \Omega^+, \quad (1c)$$

$$\ddot{\mathbf{u}}_e \cdot \mathbf{n} = \ddot{\mathbf{u}}_f \cdot \mathbf{n} = -\frac{1}{\rho_f} p_n^t \quad \text{on } \Gamma, \quad (1d)$$

$$(\boldsymbol{\sigma}(\mathbf{u}_e) \cdot \mathbf{n}) \times \mathbf{n} = 0 \quad \text{on } \Gamma, \quad (1e)$$

$$\boldsymbol{\sigma}(\mathbf{u}_e) \cdot \mathbf{n} = -p^t \mathbf{n} \quad \text{on } \Gamma, \quad (1f)$$

$$p^s \text{ satisfies a radiation condition at infinity,} \quad (1g)$$

where subscripts e and f denote quantities pertaining to the elastic solid and the fluid, respectively; ρ denotes density and c is the speed of sound in the fluid; \mathbf{u} denotes displacement vectors, while $\boldsymbol{\sigma}$ denotes the stress tensor, \mathbf{E} the strain tensor and \mathbf{C} the elasticity tensor for the solid; $p^t = p^s + p^0$ is the total pressure field with p^s denoting the scattered pressure field and p^0 an incident pressure field; \mathbf{n} denotes the outward normal to Γ . Equation (1a) is the equation of motion for the solid in the absence of body forces, eqn. (1b) is the constitutive law for the solid, eqn. (1c) is the scalar wave equation for the scattered pressure in the fluid, eqn. (1d) ensures that the normal velocity of the fluid is continuous across Γ , eqn. (1e) and (1f) represent the continuity of normal and tangential tractions across Γ respectively. Given p^0 and some appropriate initial conditions, eqs. (1a)–(1g) represent the strong form of the fluid–structure interaction problem. Following Everstine [12] and based on the assumption of irrotational flow, the scattered fluid velocity field can be expressed as the gradient of a potential ψ , thus leading to:

$$p^s = -\rho_f \dot{\psi}. \quad (2)$$

With the introduction of the velocity potential ψ , eqns. (1c), (1d) and (1f) can be replaced by:

$$\begin{aligned} \nabla^2 \psi &= \frac{1}{c^2} \ddot{\psi} \quad \text{in } \Omega^+, & \dot{\mathbf{u}}_e \cdot \mathbf{n} &= \dot{\psi}_n - \frac{1}{\rho_f} \int_0^t p_n^0 \, d\tau \quad \text{on } \Gamma, \\ \boldsymbol{\sigma}(\mathbf{u}_e) \cdot \mathbf{n} &= (-p^0 + \rho_f \dot{\psi}) \mathbf{n} \quad \text{on } \Gamma. \end{aligned} \quad (3)$$

Since the scattered wave $-\rho_f \dot{\psi}$ must be outgoing, then it is ψ that must satisfy the radiation condition at infinity instead of p^s .

Now, rather than considering the structural acoustic scattering problem over the infinite domain Ω^+ , we introduce an artificial, smooth, convex boundary Γ_a in Ω^+ and pose a problem equivalent to (1) over the finite region $\Omega^e \cup \bar{\Omega}^f$ [Fig. 1(b)]. Then on Γ_a , ψ will satisfy an exact non-local condition for the normal derivative, which symbolically can be expressed as:

$$\psi_n = \mathcal{F}[\psi] \quad \text{on } \Gamma_a. \quad (4)$$

\mathcal{F} above, is the exact operator, which merely expresses the fact that the motion at every point on the artificial boundary Γ_a is coupled with the time histories of all other points on Γ_a . Equations (1a)–(1b), (3) and (4) represent the modified strong form of the fluid–structure interaction problem (with appropriate initial conditions). The corresponding weak form can

then be stated as follows: Given an incident pressure field p^0 and appropriate initial conditions, find \mathbf{u}_e and ψ so that for all admissible pairs $(\delta\mathbf{u}, \delta\psi)$, the following holds:

$$\int_{\Omega^e} \nabla \mathbf{u}_e : \mathbf{C} : \nabla \delta \mathbf{u} \, d\Omega^e + \rho_e \int_{\Omega^e} \delta \mathbf{u} \cdot \ddot{\mathbf{u}}_e \, d\Omega^e - \rho_f \int_{\Gamma} \dot{\psi} \delta \mathbf{u} \cdot \mathbf{n} \, d\Gamma + \int_{\Gamma} p^0 \delta \mathbf{u} \cdot \mathbf{n} \, d\Gamma = 0, \quad (5a)$$

$$\begin{aligned} & -\rho_f \int_{\Omega^f} \nabla \delta \psi \cdot \nabla \psi \, d\Omega^f - \frac{\rho_f}{c^2} \int_{\Omega^f} \delta \psi \ddot{\psi} \, d\Omega^f - \rho_f \int_{\Gamma} \delta \psi \dot{\mathbf{u}}_e \cdot \mathbf{n} \, d\Gamma - \int_{\Gamma} \delta \psi \int_0^t p_n^0 \, d\tau \, d\Gamma \\ & + \rho_f \int_{\Gamma_a} \delta \psi \mathcal{F}[\psi] \, d\Gamma_a = 0. \end{aligned} \quad (5b)$$

Notice that eqs. (5a) and (5b), upon discretization, will yield a symmetric system of equations, provided that the last term of eqn. (5b), which corresponds to the contribution of the absorbing boundary Γ_a , can also be cast in symmetric terms.

The absorbing boundary

In order to reduce the non-local character of \mathcal{F} , one seeks to approximate \mathcal{F} , aiming in particular at reducing the temporal non-locality. Barry et al. [13] obtained a family of approximations of increasing accuracy and complexity of \mathcal{F} . The first three are:

$$\psi_n = -\frac{1}{c} \dot{\psi}, \quad (6a)$$

$$\psi_n = -\frac{1}{c} \dot{\psi} + \frac{1}{2} \kappa \psi, \quad (6b)$$

$$\dot{\psi}_n + \delta \psi_n = -\frac{1}{c} \ddot{\psi} + \left(\frac{1}{2} \kappa - \frac{\delta}{c} \right) \dot{\psi} + \frac{1}{2} c \psi_{\lambda\lambda} + \left(\frac{1}{8} \kappa^2 c + \frac{1}{2} k \delta \right) \psi, \quad (6c)$$

in which the subscript λ denotes differentiation with respect to the arc length, κ is the curvature of Γ_a and δ is a stability parameter. All three conditions are appropriate candidates for replacing the exact operator \mathcal{F} in eqn. (5b); for reasons of increased accuracy and economy (reduced computational domain) as evidence in [14], we seek to implement eqn. (6c). The other two are straightforward. The apparent difficulty of eqn. (6c) is that it contains a linear combination of both ψ_n and its time derivative $\dot{\psi}_n$, as opposed to eqs. (6a) and (6b) which contain only ψ_n . Naturally, one can approximate $\dot{\psi}_n$, but the resulting time-marching scheme destroys the symmetry, and possibly the accuracy, of the original formulation. By introducing two auxiliary variables $\psi^{(1)}$ and $\psi^{(2)}$ on Γ_a , it can be shown [14], that eqn. (6c) can be rewritten as the following system of three equations:

$$\begin{aligned} \psi_n &= -\frac{1}{c} \dot{\psi} + \frac{\kappa}{2} \psi + \frac{\kappa^2 c}{8\delta} \psi^{(1)} + \frac{c}{2\delta} \psi_{\lambda\lambda}^{(2)}, \\ \psi - \psi^{(1)} &= \frac{1}{\delta} \dot{\psi}^{(1)}, \quad \psi_{\lambda\lambda} - \psi_{\lambda\lambda}^{(2)} = \frac{1}{\delta} \dot{\psi}_{\lambda\lambda}^{(2)}. \end{aligned} \quad (7)$$

In light of eqn. (7), the last term in eqn. (5b) can now be written as:

$$\begin{aligned} -\int_{\Gamma_a} \delta \psi \mathcal{F}[\psi] \, d\lambda &\approx \int_{\Gamma_a} \left(\frac{1}{c} \dot{\psi} - \frac{\kappa}{2} \psi - \frac{\kappa^2 c}{8\delta} \psi^{(1)} \right) \delta \psi \, d\lambda + \int_{\Gamma_a} \frac{c}{2\delta} \psi_{\lambda}^{(2)} \delta \psi_{\lambda} \, d\lambda \\ &\quad - \int_{\Gamma_a} \frac{\kappa^2 c}{8\delta} \left(\psi - \psi^{(1)} - \frac{1}{\delta} \dot{\psi}^{(1)} \right) \delta \psi^{(1)} \, d\lambda \\ &\quad + \int_{\Gamma_a} \frac{c}{2\delta} \left(\psi_{\lambda} - \psi_{\lambda}^{(2)} - \frac{1}{\delta} \dot{\psi}_{\lambda}^{(2)} \right) \delta \psi_{\lambda}^{(2)} \, d\lambda. \end{aligned} \quad (8)$$

It is important to notice that the substitution of eqn. (8) into eqn. (5b) will yield a symmetric system of equations. Furthermore, as the time derivatives involved in eqn. (8) are at most of first order, the addition of the absorbing boundary will also maintain the order of the resulting system of differential equations, by contributing to the stiffness and damping of the original system. The cost of the additional degrees of freedom on the boundary is minimal. It is also important to notice that the form of eqn. (8) is independent of the particular formulation for the fluid presented herein; indeed, had we chosen to formulate the fluid–structure interaction problem in terms of the pressure in the fluid region, the resulting unsymmetric form could equally use eqn. (8), provided that ψ above were replaced by the total pressure p^t .

Finite element discretization

Standard finite element polynomial approximations are used for the spatial discretization of eqn. (5), namely for approximating the displacement vector \mathbf{u}_e , the potential ψ and their respective test functions. Here we concentrate on the discretization of the absorbing boundary, i.e. of eqn. (8). To this end, we introduce for quantities on Γ_a :

$$\begin{aligned} \psi(\mathbf{x}, t) &= \boldsymbol{\alpha}^T(\mathbf{x})\psi_{\Gamma_a}(t), & \psi^{(1)}(\mathbf{x}, t) &= \boldsymbol{\beta}^T(\mathbf{x})\psi^{(1)}(t), & \psi_\lambda^{(2)}(\mathbf{x}, t) &= \boldsymbol{\gamma}^T(\mathbf{x})\eta(t), \\ \delta\psi(\mathbf{x}) &= \delta\psi^T\boldsymbol{\alpha}(\mathbf{x}), & \delta\psi^{(1)}(\mathbf{x}) &= \delta\psi^{(1)T}\boldsymbol{\beta}(\mathbf{x}), & \delta\psi_\lambda^{(2)}(\mathbf{x}) &= \delta\eta^T\boldsymbol{\gamma}(\mathbf{x}), \end{aligned} \quad (9)$$

$$(10)$$

in which, $\boldsymbol{\alpha}$, $\boldsymbol{\beta}$ and $\boldsymbol{\gamma}$ are vectors of global shape functions; ψ , $\psi^{(1)}$ and η are the unknown nodal values defined over Γ_a , initially at rest. Notice that in eqn. (9) we approximate the tangential derivative $\psi_\lambda^{(2)}$ instead of $\psi^{(2)}$ in order to avoid singular matrices in later calculations. Taking κ and δ to be constant over each element and by virtue of eqn. (9) and (10), eqn. (8) leads to a discretized representation for an element on Γ_a as:

$$\begin{aligned} - \int_{\Gamma_a^e} \delta\psi \mathcal{F}[\psi] \delta\lambda &\approx \begin{bmatrix} -\frac{\kappa}{2}\mathbf{k}_{11} & -\frac{\kappa^2 c}{8\delta}\mathbf{k}_{12} & \frac{c}{2\delta}\mathbf{k}_{13} \\ -\frac{\kappa^2 c}{8\delta}\mathbf{k}_{12}^T & \frac{\kappa^2 c}{8\delta}\mathbf{k}_{22} & 0 \\ \frac{c}{2\delta}\mathbf{k}_{13}^T & 0 & -\frac{c}{2\delta}\mathbf{k}_{33} \end{bmatrix} \begin{bmatrix} \psi_{\Gamma_a^e} \\ \psi^{(1)} \\ \eta \end{bmatrix} \\ &+ \begin{bmatrix} \frac{1}{c}\mathbf{k}_{11} & 0 & 0 \\ 0 & \frac{\kappa^2 c}{8\delta^2}\mathbf{k}_{22} & 0 \\ 0 & 0 & -\frac{c}{2\delta^2}\mathbf{k}_{33} \end{bmatrix} \begin{bmatrix} \dot{\psi}_{\Gamma_a^e} \\ \dot{\psi}^{(1)} \\ \dot{\eta} \end{bmatrix}, \end{aligned}$$

with

$$\begin{aligned} \mathbf{k}_{11} &= \int_{\Gamma_a^e} \boldsymbol{\alpha}\boldsymbol{\alpha}^T d\lambda, & \mathbf{k}_{22} &= \int_{\Gamma_a^e} \boldsymbol{\beta}\boldsymbol{\beta}^T d\lambda, & \mathbf{k}_{33} &= \int_{\Gamma_a^e} \boldsymbol{\gamma}\boldsymbol{\gamma}^T d\lambda, \\ \mathbf{k}_{12} &= \int_{\Gamma_a^e} \boldsymbol{\alpha}\boldsymbol{\beta}^T d\lambda, & \mathbf{k}_{13} &= \int_{\Gamma_a^e} \boldsymbol{\alpha}_\lambda\boldsymbol{\Gamma}^T d\lambda, \end{aligned} \quad (11)$$

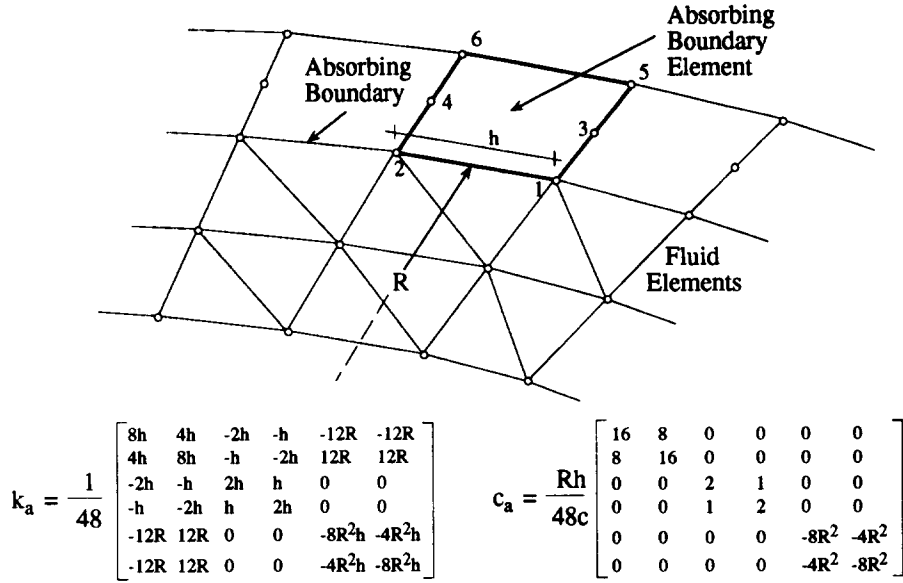


Fig. 2. Absorbing boundary element geometry; linear element stiffness and damping matrices.

where Γ_a^c denotes an element on Γ_a . The first of the two matrices in (11) is a stiffness-like contribution to the global stiffness of the system, while the second matrix in (11) is a damping-like contribution. A representative geometry of the absorbing boundary element is shown in Fig. 2 for the case of a circular absorbing boundary of radius R which is approximated by linear elements; the corresponding element stiffness (k_a) and damping (c_a) matrices, also included in Fig. 2, were obtained using $\delta = c/R$; this value makes the absorbing boundary condition used herein coincide for the case of a circle with the second-order condition of Bayliss and Turkel [8]. It should also be noted that in Fig. 2, the actual distance between nodes 1 and 2 and any of 3–6 is immaterial to the formulation.

Once eqn. (11) is introduced into the discretized form of eqn. (5) there results a system of ordinary differential equations with the following structure:

$$M\ddot{U} + C\dot{U} + KU = F, \tag{12}$$

where $U^T = (u_c^T, \psi_\Gamma^T, \psi_{\Omega^f}^T, \psi_{\Gamma_a}^T, \psi^{(1)T}, \eta^T)$, ψ_Γ , ψ_{Ω^f} and ψ_{Γ_a} are partitions of ψ over Γ , Ω^f , and Γ_a respectively, M , C and K are the mass, damping, and stiffness matrices of the system, and $F(t)$ represents the effective wave excitation. The coupling between the structure and the fluid is represented via off-diagonal terms of the damping matrix as it can readily be seen from the third terms in eqs (5a) and (5b). Equation (12) can be solved using standard time integration schemes; for the numerical results obtained herein the trapezoidal rule was used. The same equation can be used for steady-state harmonic excitation.

Numerical results

Several infinitely long steel thin elastic shells submerged in water were considered as model cases in order to assess the validity of the proposed methodology and its implementation into existing software for interior problems. One case involves a shell with a circular cross-section, analyzed using shell theory [15], while the others deal with a shell of more complex geometry as shown in Fig. 3, together with the corresponding finite element mesh. In the latter model the shell is treated as a standard two-dimensional isotropic, homogeneous,

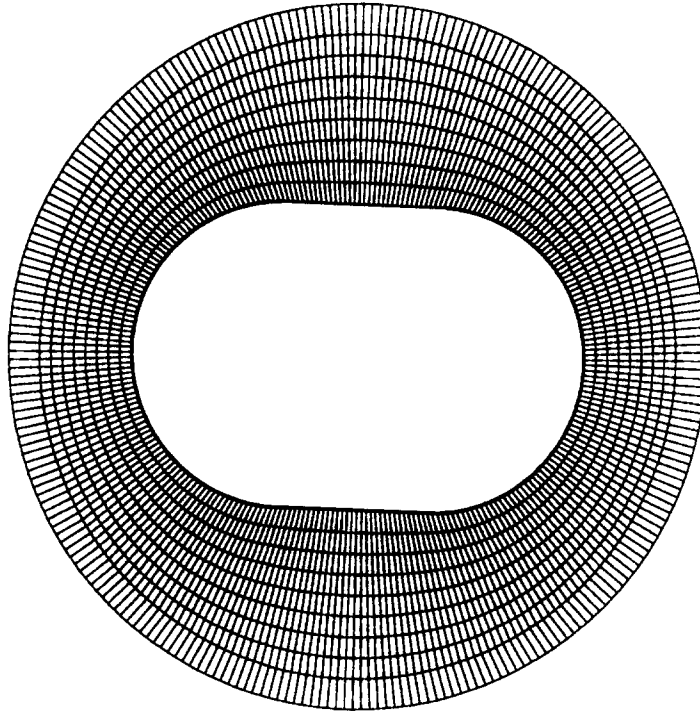


Fig. 3. Finite element mesh for a coupled shell–fluid system; ($n_r = 8$, $n_\theta = 256$).

elastic medium. The relative properties, in all cases, are: $c_s/c = 3.53$, $\rho_s/\rho_f = 7.65$, $\nu = 0.3$ and $d/a = 0.01$, where c_s is the velocity of compressional waves in the shell, ν is Poisson's ratio, d is the thickness and a a characteristic length of the shell (radius in the case of circular shells). We considered an exterior excitation in the form of a traveling plane wave that impinges normally upon the axis of the shell (two-dimensional scattering problem). In all cases the time signal was represented by a finite-duration modified Ricker pulse. The Ricker pulse has the property that the amplitude of its Fourier transform has a single well-defined

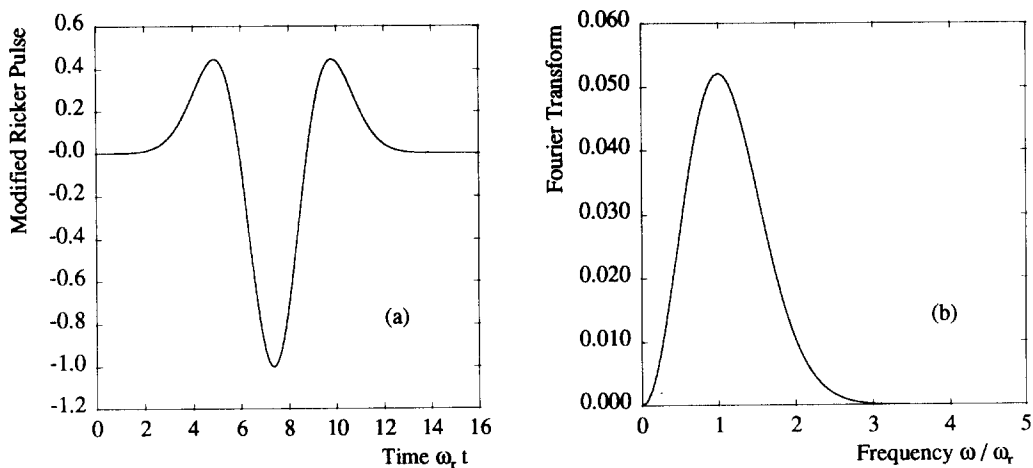


Fig. 4. Modified Ricker pulse (a) and its Fourier transform (b).

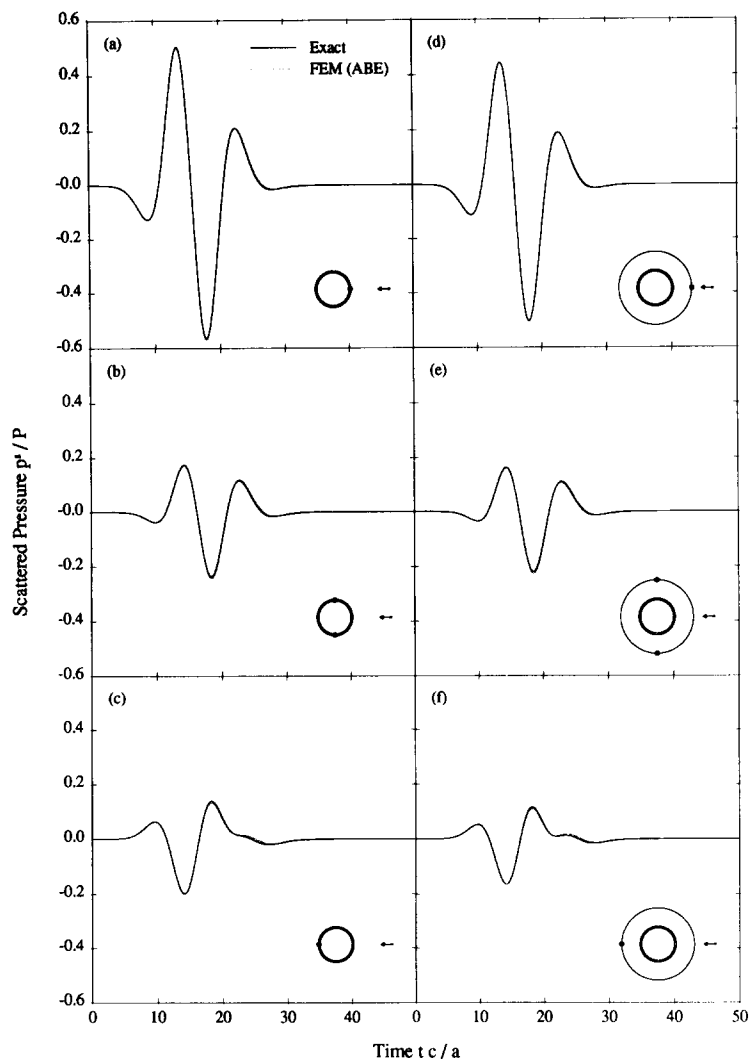


Fig. 5. Scattered pressure due to a plane wave impinging on a circular cylindrical shell; $k_r a = 0.5$; FEM solution with $n_r = 2$, $n_\theta = 16$, $r/a = 1.2$; (a, b, c) points on the surface of the shell; (d, e, f) points on the absorbing boundary.

central frequency ω_r and has non-zero values only over a narrow frequency band. The excitation, normalized to a unit amplitude, and its transform are shown in Fig. 4(a) and 4(b) for a dominant frequency $\omega_r = 1$.

Figure 5 depicts the scattered pressure computed at different points, marked by solid bullets, on the surface of a circular cylindrical shell of radius a and on the absorbing boundary. The shell is illuminated by a plane wave of unit amplitude traveling along the direction of the arrow (from east to west); the time signal of the exciting wave has a dominant frequency $\omega_r = 0.5$ (or a dimensionless wave number $k_r a = 0.5$). There are two curves per graph; the dotted line represents the FEM solution which was obtained by using the formulation and the absorbing boundary element (ABE) described herein. The solid curve, marked exact, represents the exact time domain solution obtained by inversion (via FFTs) of the exact frequency domain solution. For the FEM solution, the absorbing boundary was placed at a distance of $1.2a$, i.e. at only $0.2a$ from the surface of the shell; we used 2

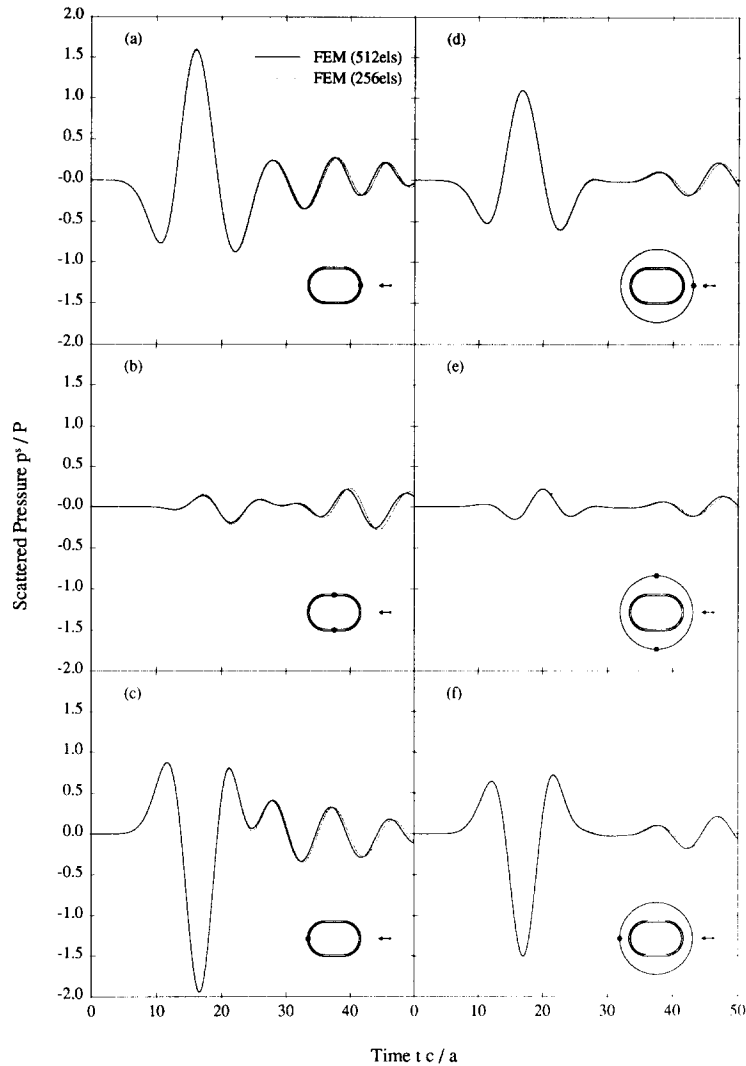


Fig. 6. Scattered pressure due to a plane wave impinging on the shell; $k_r a = 0.5$; FEM solution with $n_r = 8$, $n_\theta = 256$ and 512, $r/a = 0.6$; (a, b, c) points on the surface of the shell; (d, e, f) points on the absorbing boundary.

quadratic elements along the radial direction ($n_r = 2$) and 16 quadratic elements along the circumferential direction ($n_\theta = 16$). As it can be seen, each curve is indistinguishable from the other at all locations.

In Fig. 6 we consider the non-circular shell shown in Fig. 3; the outermost layer of elements in Fig. 3 represents ABEs. Here a is the radius of the semicircular sections of the shell as well as the distance between their centers. The excitation is again a Ricker pulse with a dominant wavenumber, $k_r a$, equal to 0.5. The absorbing boundary was placed at $0.6a$ from the shell's rightmost edge and the FEM solutions were obtained using a specially modified version of a commercial code (ANSYS). The two curves shown were obtained using different mesh densities; in both cases we used 8 linear elements along the radial direction, while 512 (solid line) and 256 (dotted line) linear elements were used along the circumferential direction. The large number of elements in the circumferential direction is needed in order to

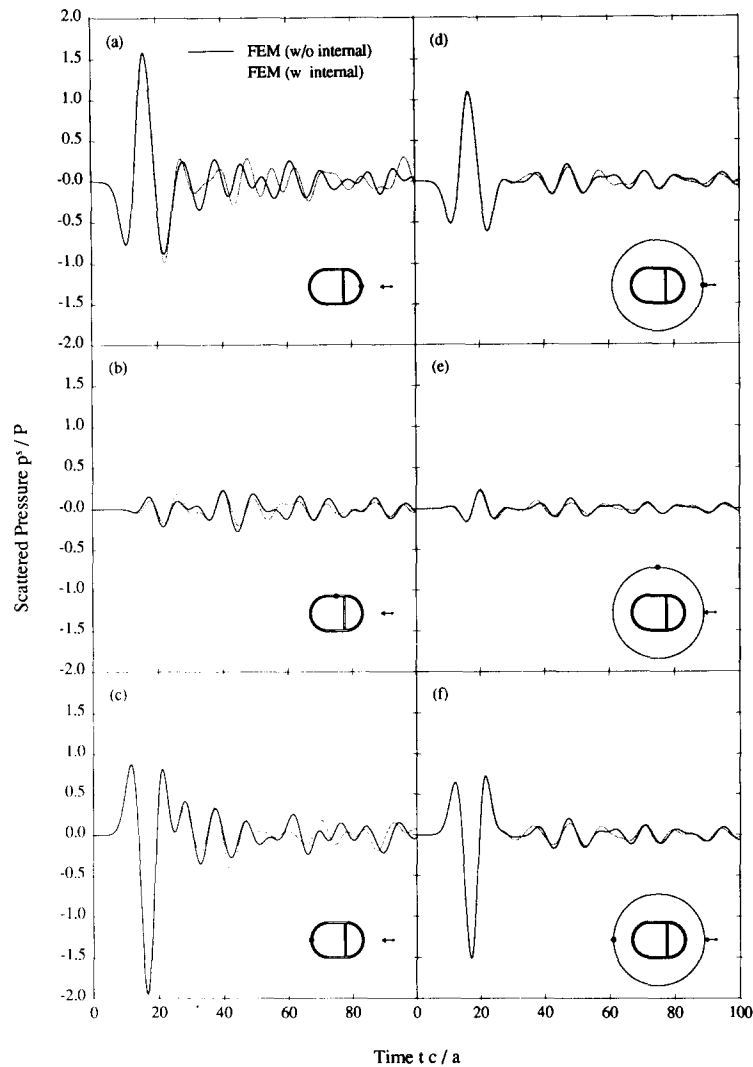


Fig. 7. Scattered pressure due to a plane wave impinging on a shell with and without an internal; $k_r a = 0.5$; FEM solution with $n_r = 8$, $n_\theta = 256$, $r/a = 0.6$; (a, b, c) points on the surface of the shell; (d, e, f) points on the absorbing boundary.

characterize the higher modes excited by the incident wave. To examine the effect of the absorbing boundary on the solution, we solved the problem again with the boundary placed at $1.2a$, using 512 angular elements and 12 radial elements, without change in the results; hence the solid line can be essentially regarded as an exact solution.

To illustrate the behavior of a more complex system, in Fig. 7 we consider again the shell shown in Fig. 3 with the addition of an internal elastic plate placed across the diameter of the right semicircular section and clamped to the shell. The thickness of the plate is the same as that of the shell. The excitation is provided, as before, by a Ricker wavelet with a central wavenumber, $k_r a$, equal to 0.5. The solid line shown in Fig. 7 corresponds to the shell without the internal plate while the dotted line corresponds to the same shell with the internal plate. Both curves were obtained by using linear elements, namely 256 angular and 8 radial elements. The absorbing boundary was placed at $0.6a$ from the shell's rightmost edge. It can be seen that the presence of the internal plate clearly alters the scattered pressure field.

Conclusions

In light of the numerical results, it appears that the proposed methodology based on finite element spatial discretization, standard step-by-step time integration and the absorbing boundary element (ABE) is well suited for tackling efficiently and accurately complex transient radiation and scattering problems in structural acoustics directly in the time domain. The methodology can also be used in the frequency domain either directly by solving eqn. (12) in the presence of harmonic loads, or indirectly by applying FFTs on the time domain responses. The higher-order condition which is embedded in the ABE, is more accurate (for the same position) than the often used lower-order conditions, and thus results in greater economy, as the size of the computational domain can be drastically reduced. At the same time, the higher-order condition also performs better than the lower approximations in the presence of higher modes; the reason lies with its spatial weakly non-local character. Since the ABE can be completely defined by a pair of symmetric stiffness and damping matrices, it lends itself to easy incorporation into existing finite element codes originally written for interior problems. It should also be noted that the structure of the ABE's matrices is independent of the formulation (potential-based) followed herein; these matrices can be equally used with a pressure-based formulation. The entire procedure is also amenable to ready parallelization that will best exploit advanced architecture computers, as the ABE retains the symmetry and sparsity of the overall system of equations.

The formulation was herein restricted to the analysis of elastic structures submerged in full space. The treatment of the infinite fluid, however, can be applied without modification to analyze a possible inelastic structure submerged in a half-space, provided the problem conditions are such that the fluid can still be idealized as a linear acoustic medium.

Acknowledgement

The work of L.F. Kallivokas was supported by a fellowship from Swanson Analysis Systems, Inc., We are grateful for this support.

References

- [1] R.A. JEANS and I.C. MATHEWS, "Solution of fluid–structure interaction problems using a coupled finite element and variational boundary element technique", *J. Acoust. Soc. Am.* **88**(5), pp. 2459–2466, 1990.
- [2] A.J. BURTON and G.F. MILLER, "The application of integral equation methods to the numerical solution of some exterior boundary-value problems", *Proc. Roy. Soc. Lond.* **323A**, pp. 201–210, 1971.
- [3] H.A. SCHENCK, "Improved integral formulation for acoustic radiation problems", *J. Acoust. Soc. Am.* **44**, pp. 41–58, 1967.
- [4] D. GIVOLI, "Non-reflecting boundary conditions: a review", *J. Comput. Phys.* **94**(1), pp. 1–29, 1991.
- [5] T.L. GEERS and C.A. FELIPPA, "Doubly asymptotic approximations for vibration analysis of submerged structures", *J. Acoust. Soc. Am.* **73**(4), pp. 1152–1159, 1983.
- [6] P.M. PINSKY, L.L. THOMPSON and N.N. ABBOUD, "Local high-order radiation boundary conditions for the two-dimensional time-dependent structural acoustics problem", *J. Acoust. Soc. Am.* **91**(3), pp. 1320–1335, 1992.
- [7] P.M. PINSKY and N.N. ABBOUD, "Transient finite element analysis of the exterior structural acoustics problem", *ASME J. Vib. Acoust.* **112**, pp. 245–256, 1990.
- [8] A. BAYLISS and E. TURKEL, "Radiation boundary conditions for wave-like equations", *Commun. Pure Appl. Math.* **33**(6), pp. 707–725, 1980.
- [9] T.L. GEERS and P. ZHANG, "Doubly asymptotic approximations for internal and external acoustic domains: formulation", *Winter Annu. Meeting, ASME*, Dec. 1991.
- [10] T.L. GEERS and YEN Chi-Lin, "Inelastic response of an infinite cylindrical shell to transient acoustic waves", *ASME J. Appl. Mech.* **56**, pp. 900–909, 1989.

- [11] L.F. KALLIVOKAS and J. BIELAK, “Time-domain analysis of transient structural acoustics problems based on the finite element method and a novel absorbing boundary element”, *J. Acoust. Soc. Am.*, 1993 (accepted for publication).
- [12] G.C. EVERSTINE, “A symmetric potential formulation for fluid–structure interaction”, *J. Sound Vibr.* **79**(1), pp. 157–160, 1981.
- [13] A. BARRY, J. BIELAK and R.C. MACCAMY, “On absorbing boundary conditions for wave propagation”, *J. Comput. Phys.* **79**, pp. 449–468, 1988.
- [14] L.F. KALLIVOKAS, J. BIELAK and R.C. MACCAMY, “Symmetric local absorbing boundaries in time and space”, *ASCE J. Eng. Mech.* **117**(9), pp. 2027–2048, 1991.
- [15] M.C. JUNGER and D. FEIT, *Sound, Structures, and Their Interaction*, MIT Press, Cambridge, MA, 1972.